

*In Nanoengineering: Fabrication, properties, optics, and devices II, edited by E.A. Dobry and L.A. Elklada, Proc. SPIE 5931, Optics & Photonics 31 July - 4 August 2005, San Diego CA*

## Toward hot-hole THz lasers in homoepitaxial Si and GaAs with layered doping

M. V. Dolguikh,<sup>a)</sup> A.V. Muravjov,<sup>a)</sup> R. E. Peale,<sup>a)</sup> R. A. Soref,<sup>b)</sup> D. Bliss,<sup>b)</sup> C. Lynch,<sup>b)</sup> and D. W. Weyburne<sup>b)</sup>

<sup>a)</sup> Dept. of Physics, University of Central Florida, Orlando FL, 32816-2385

<sup>b)</sup> Sensors Directorate, Air Force Research Lab., Hanscom AFB, MA 01731

### ABSTRACT

A recently proposed THz laser concept in homoepitaxially grown p-Ge with layered doping is reviewed. Prospects for realizing a similar design in Si or GaAs are considered.

**Keywords:** terahertz, far infrared, laser, germanium, silicon, gallium arsenide, epitaxy.

### INTRODUCTION

Recent terahertz semiconductor-laser developments include inter-subband p-Ge lasers [1], lasers based on optically-pumped donors in Si [2], quantum cascade lasers (QCL) [3-5], and proposed p-type Si/SiGe quantum cascade lasers [6]. All of them suffer from a rapid increase in far-IR lattice absorption with temperature [7], to offset which requires higher gain and hence higher active carrier concentration, until the population inversion becomes negatively impacted by impurity and carrier-carrier scattering. QCLs have achieved continuous-wave (CW) output and operation temperatures above liquid nitrogen via a design with extreme tolerances that requires growth by molecular beam epitaxy (MBE). This limits QCL active layer thickness to  $\sim 10 \mu\text{m}$ , which is less than the generated wavelength, requiring complex and lossy cavity solutions. The only working THz QCLs have been based on AlGaAs-GaAs multi-quantum wells.

### GERMANIUM TERAHERTZ LASERS

Among all semiconductor terahertz lasers listed above, only p-Ge lasers have demonstrated a wide tuning range. Three distinct mechanisms of laser emission have been realized experimentally in p-Ge. The intervalence band (IVB) mechanism (1 W peak power) can be tuned over the range  $50\text{-}140 \text{ cm}^{-1}$  using intracavity selectors, as shown in Fig. 1. The light hole cyclotron resonance (LHCR) mechanism (100 mW peak power) is magnetically tunable over the range  $30\text{-}100 \text{ cm}^{-1}$ . And, the heavy hole cyclotron resonance maser (10 mW peak power), also known as the negative effective mass amplifier and generator (NEMAG), is magnetically tunable from 40 to 400 GHz. In this paper, we will briefly review the first two of these mechanisms and a modification of the p-Ge gain medium that promises to enhance the gain. Then we will consider the potential of these approaches in Si and GaAs.

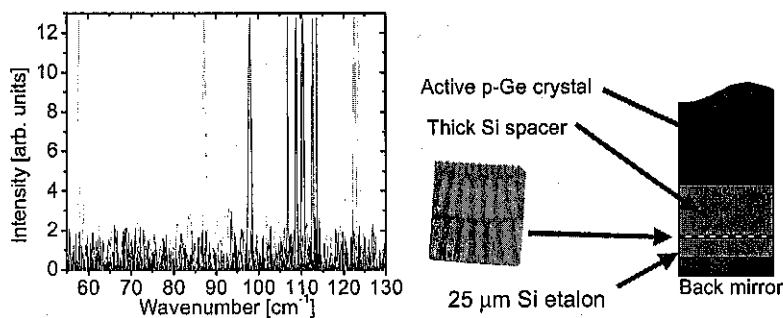


Fig. 1. (Left) Narrow-line spectra for p-Ge laser with different intracavity wavelength selectors. Achieved line width is  $0.1 \text{ cm}^{-1}$ . (Right) Intracavity etalon with diffraction structure used to select laser emission wavelength.

For the IVB and LHCR mechanisms, the inverted population grows at certain ratios of applied crossed electric and magnetic fields, when light holes are accumulated on closed trajectories below the optical phonon energy, while heavy holes undergo rapid optical phonon scattering. Fig. 2 is a schematic quasi-classical explanation of the IVB laser mechanism that is valid at low applied fields where Landau-level spacing is much less than carrier kinetic energy.

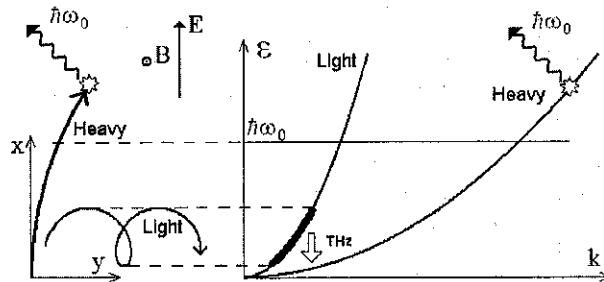


Fig. 2. Schematic of quasi-classical explanation for intersubband hot-hole laser.

At magnetic fields above 3 T, quantization of the spectrum becomes important, and mixing between light and heavy sub-bands by the fields allows population inversion and lasing transitions between Landau levels within the light subband itself, the LHCR mechanism. LHCR lasers produce a narrow line whose frequency is proportional to the applied magnetic field. Due to the constraints of free-carrier and lattice absorption, the tuning range 30-100  $\text{cm}^{-1}$  is similar to that for the intervalence band mechanism (50-140  $\text{cm}^{-1}$ ), as explained below. The light-hole Landau levels are populated by the same scattering mechanism depicted in Fig. 2.

Light hole life time, responsible for the inversion population and for the gain, is determined by acoustic phonon scattering, ionized impurity scattering, and carrier-carrier interaction, such that p-Ge laser operation has been limited to liquid helium temperatures and low carrier concentrations ( $\sim 10^{14} \text{ cm}^{-3}$ ). Fig. 3 (left) shows that the limit to the doping concentration, and therefore the gain, is due to a steep decrease in gain cross section as a consequence of impurity scattering on ionized acceptor centers.

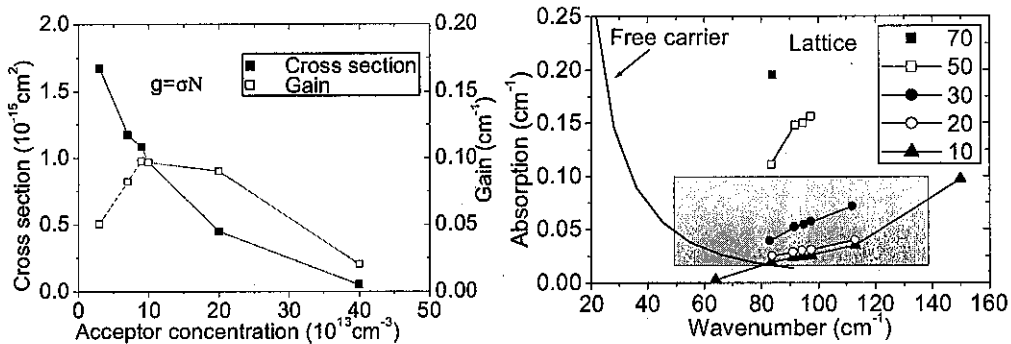


Fig. 3 (Left). Calculated gain cross section  $\sigma$  and gain  $g$  for the p-Ge laser as a function of carrier concentration  $N$ . Due to ionized impurity scattering by the acceptors, which are the source of holes, the gain is optimized at the rather low concentration value of  $\sim 10^{14} \text{ cm}^{-3}$ , which agrees with experiment. (Right) Experimental temperature-dependent lattice absorption (symbols) and free carrier absorption (smooth curve) for  $\sim 10^{14} \text{ cm}^{-3}$  hole concentration. The legend gives temperature in K. The shaded box gives the range of gain and emission-wavenumbers reported for intervalenceband p-Ge lasers. It is clear that the limited gain in combination with intrinsic absorption determine the tuning range and maximum operating temperature.

Fig. 3 results show that small signal gain in p-Ge lasers usually does not exceed  $0.1 \text{ cm}^{-1}$ . As shown in Fig. 3 (right), this is smaller than the Ge lattice absorption at 50 K [7]. Thus the maximum operating temperature is limited by intrinsic lattice absorption in the active crystal. Because of Joule heating during electrical pumping, the duty cycle of the bulk p-Ge laser is similarly limited. The maximum

gain value, and the spectral dependence of the lattice and free carrier absorption, limit tuning to the range 50-140  $\text{cm}^{-1}$ , as shown in Fig. 3 (right).

We recently developed a terahertz laser concept based on inter-subband transitions of holes with transport in crossed electric  $E$  and magnetic  $B$  fields in a planar periodically doped p-Ge/Ge structure [8-11]. The design, shown schematically in Fig. 4, achieves spatial separation of hole accumulation regions from the doped layers, which reduces ionized-impurity scattering and carrier-carrier scattering for the majority of light holes, allowing significant increase of total carrier concentration without affecting light hole life time. The resulting increase in gain over the bulk p-Ge laser promises to raise maximum operation temperatures to 77 K. At the same time the proposed laser retains the intersubband mechanism with its wide tuning range 1-4 THz. Moreover, this crystalline-Ge device can be grown by chemical vapor deposition (CVD), which allows active thicknesses comparable to the THz wavelength, thus allowing low-loss quasi-optical cavity solutions. As soon as we have developed a THz laser concept based on CVD epitaxial Ge devices, it becomes very interesting to consider the possibility of realizing a Si THz laser because of the tremendous potential benefits of integration with Si electronics. Likewise, a similar structure based on GaAs is interesting because of the highly sophisticated technology available for epitaxial growth of this material.

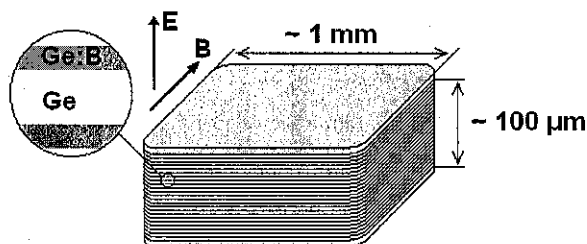


Fig. 4. Homoepitaxial multilayer Ge/p-Ge THz laser concept [8-11]. The layer period is chosen to be 300–500 nm, which is larger than the light hole cyclotron orbit, but smaller than that for heavy holes. The doped layers are  $\sim 10\%$  as thick as the period. Light holes are shown by Monte Carlo simulation to accumulate in the undoped layers where their life time is enhanced by reduced impurity scattering. This scheme allows much higher average carrier concentrations than for uniformly doped bulk, giving a corresponding increase in gain. The total stack thickness that has been achieved experimentally by chemical vapor deposition is  $\sim 30$  microns, and physical analysis suggest that 100 micron total thickness for the active region is feasible, giving a low-loss quasioptical cavity solution. A similar device with horizontal transport has also been studied.

## SILICON TERAHERTZ LASERS

We now consider the possibility of inter-valence-band and LHCR mechanisms of population inversion and stimulated emission in p-type silicon. When implemented, this would be the first crystalline-Si electrically-excited THz laser. This device differs from prior THz laser approaches because it is not a cascade and does not use transitions between impurity levels. Silicon has a number of potential advantages over germanium. The Debye frequency for Si ( $448 \text{ cm}^{-1}$ ) is much higher than that of Ge ( $260 \text{ cm}^{-1}$ ). Hence, the density of states function for phonons in Si is shifted toward higher energy relative to Ge, and the region of high optical transparency at finite temperatures, where multiphonon absorption competes with gain, is similarly shifted to higher energies. Thus Si has high transparency up to 10 THz ( $333 \text{ cm}^{-1}$ ), while Ge (Fig. 3) becomes too strongly absorbing to sustain IVB lasing already at 4.2 THz ( $140 \text{ cm}^{-1}$ ). The experimental temperature-dependent absorption spectrum of Si [12] supports this claim. An additional feature observed is that the temperature dependence of the absorption in Si is weaker, so that Si remains highly transparent even at 78 K, in stark contrast to Ge (Fig. 3).

Previous attempts to achieve lasing in p-Si have achieved spontaneous emission from population-inverted hot holes on intersubband transitions [13], but lasing has been elusive due to a number of complications. The orientation of the applied fields is much more critical for Si than for Ge because the silicon valence band is strongly anisotropic. Fig. 5 presents calculated constant energy surfaces in 3-dimensional momentum space for the light and heavy hole bands. These surfaces were determined at an energy equal to the optical phonon scattering threshold from the  $6 \times 6 \text{ k}\cdot\text{p}$  Hamiltonian, whose elements are defined by wavefunctions for the heavy hole, light hole, and split-off band. The strong anisotropy is due to

mixing with the split-off band, which cannot be ignored (as often done for Ge), because the 64.8 meV optical phonon limit to carrier kinetic energy exceeds the spin-orbit splitting (43.5 meV). Calculations of accumulation volume in momentum space [14] and Monte Carlo calculations of distribution functions [15] have identified a number of promising field orientations. Quantum mechanical calculations [16] and the only experiment performed to date [13] have considered only one of these. Thus, neither theoretical nor experimental possibilities have been sufficiently explored in the quest for lasing in bulk p-Si.

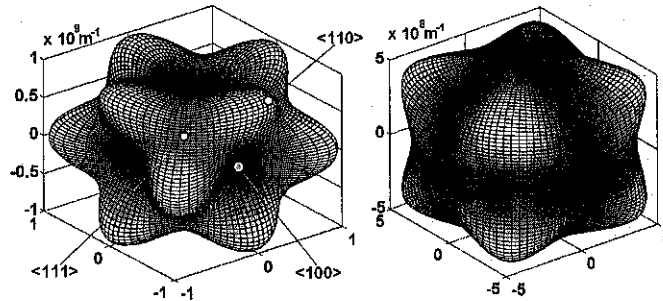


Fig. 5. Constant energy surfaces at 62 meV for heavy- (left) and light- (right) valence subbands of Si in 3-dimensional wavevector space (units of 1/m). Surfaces were calculated from the 6x6 k.p Hamiltonian, whose elements are defined by wavefunctions from the heavy hole, light hole, and split-off band.

Anisotropy results in a small energy separation between light and heavy sub-bands for  $\langle 111 \rangle$  momentum directions (Fig. 5), which leads to strong mixing of these subbands by the applied fields. This mixing is much more pronounced and complicated than in Ge. As a consequence, the average light hole lifetime is significantly lower than the estimates obtained through semiclassical calculations, due to an enhanced probability of scattering on optical phonons caused by heavy hole admixture. This means also that the degree of light hole accumulation and therefore the gain on light-to-heavy hole transitions in Si calculated by the classical MC simulation technique are strongly overestimated, which is discouraging for the IVB mechanism in bulk p-Si.

On the other hand, population inversion between Landau levels should be stronger than in Ge, giving hope for lasing based on the LHCR mechanism. Quantum calculations for Si in crossed electric and magnetic fields reveal order-of-magnitude variations in the lifetimes of Landau levels due to differing amounts of subband mixing for different Landau levels [13]. Because of the anharmonicity of the levels caused by mixing, laser transitions need not be confined to adjacent levels. This feature, together with the high transparency of the Si lattice above 4 THz, gives the possibility of tunable laser generation in the high THz region, even at 77 K, which is impossible in Ge.

The pumping mechanism for both IVB and LHCR mechanisms is as described in Fig. 2 with strong dependence on optical phonon scattering. Optical phonon scattering in the anisotropic case of Si is also anisotropic, as shown in Fig. 6. Bir and Pikus [17] supplied all theory for deformation potential matrix elements in 6\*6 model. The results of the calculation are presented in Fig. 6. For  $\langle 100 \rangle$  crystallographic orientation the scattering rate is about 1.5 times higher than for  $\langle 110 \rangle$  ( $\langle 111 \rangle$ ) orientation for heavy (light) holes. This anisotropy in optical phonon scattered should be included in future theoretical investigations of hot-hole Si lasers, in order to intelligently choose the field orientations for experiments.

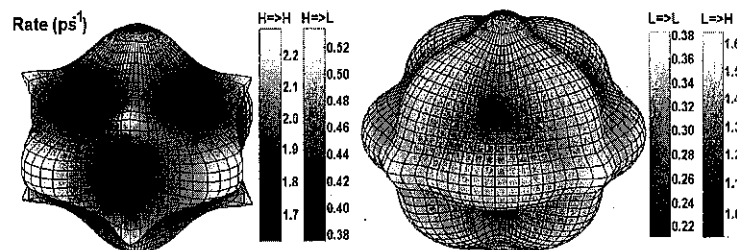


Fig. 6. Intra- and inter-subband transition rates with emission of optical phonon for heavy-hole (left) and light-hole (right) as a function of crystallographic orientation for Si. Phonon distribution  $N_q$  was set to zero (low temperature limit).

Acoustic phonon scattering is a detrimental process that disrupts the required anisotropic hole distributions. Acoustic phonon scattering rates are proportional to fundamental deformation potentials, temperature dependent phonon populations, and the density of final states for scattered holes. Fig. 7 compares the density of hole states as a function of heavy-hole energy for Si and Ge in the fully anisotropic band approximation. The density of states is significantly higher in Si. The ratio of the density of states for Ge increases with energy from 2 to 3. Ignoring differences in deformation potentials and phonon populations, the Fig. 7 result suggests that acoustic phonon scattering will be stronger in Si. This is supported by calculations of drift velocity for Si and Ge at 77 K in 1 kV/cm applied fields, which shows a slower value for Si by the factor 2.2 [18].

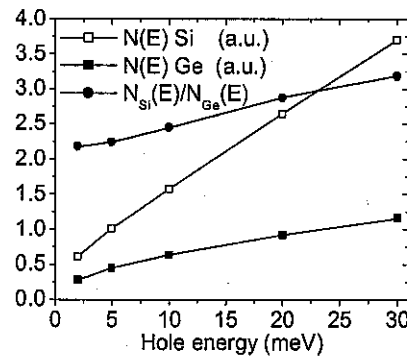


Fig. 7. Density of heavy hole states for Si and Ge vs. hole energy and their ratio.

Another challenge for Si is that the acceptor impurity levels are relatively deep in Si compared with Ge. Carriers bound at low temperature to doping levels can be liberated by a variety of effects in an applied E-field. These are shallow impurity impact ionization, Frenkel-Poole effect, tunneling, and phonon-assisted tunneling. The emission rate at 1 kV/cm and 20 K by Poole Frenkel effect is only 1000/s, i.e. millisecond emission time constants [19]. By phonon assisted tunneling, the emission rate is only 10/s, and it is much less than 1/s for straight tunneling. Thus, only the mechanism of impact ionization has potential to generate the required hole population of  $\sim 10^{14} \text{ cm}^{-3}$  within the  $\sim 100 \text{ ns}$  rise time of the  $\sim 1 \text{ kV/cm}$  excitation pulse applied to the proposed p-Si hot hole laser.

Boron in the best p-type dopant, because its 45 meV ionization energy is the smallest for acceptor impurities in Si. The only concentration value that has been explored experimentally [13] was  $5 \times 10^{15} \text{ cm}^{-3}$ , which is 2 orders of magnitude higher than the optimum value for p-Ge lasers. This choice was adopted presumably to overcome the expected lower fractional impact ionization for the deeper Si:B acceptor than occurs for the comparatively shallow Ge:Ga acceptor at 4 K. The hot-hole laser operation is quite sensitive to acceptor concentration (Fig. 3), so a wider concentration range needs to be explored.

Impact ionization is usually treated as the process of promoting a valence electron to the conduction band [20]. If one supposes that the same formulas hold for impact ionization of acceptors, with gap energy replaced by ionization energy  $E_i$  and effective mass of bound and free holes the same, then the threshold energy  $E_t$  for impact ionization is  $\sim 1.5 * E_i$ . For Ge:Ga,  $E_i = 16 \text{ meV}$ , i.e. less than half the 37 meV free hole energy limit set by optical phonon scattering. Thus, free holes can easily gain sufficient energy under electrical heating to impact ionize neutral Ga acceptors in Ge, in agreement with experiment. For Si:B,  $E_i = 67 \text{ meV}$ , which exceeds the optical phonon energy in Si of 64.8 meV. This suggests that a free hole can never gain enough energy to impact-ionize a Boron acceptor in Si. Although this picture is too simple, it illustrates the challenge that the deeper ionization threshold for acceptors in Si poses to realizing a p-Si hot hole laser. Experimentally, impact ionization does occur, at least at 20 K [21]. The threshold velocity for holes to ionize acceptors at 20 K was found to be close to the saturated velocity due to optical phonon scattering, in agreement with the simple model above. Thus, impact ionization requires rather large applied fields, at least a few 100 V/cm.

The difficulty of impact ionization for Si:B ( $p = 10^{15} \text{ cm}^{-3}$ ) even at the elevated temperature 77 K was experimentally noted very early [22]. In this work, the I-V curve was observed to be linear at 77 K even up to 10 kV/cm applied field, with no observation of the expected saturation plateau until the temperature was raised to 183 K. The explanation was as follows. Carrier freeze out in Si:B begins already

at 170 K. At 77 K, only 4% of B is ionized. So the continued increase in current with field above the expected saturation point is due to generation of additional carriers by field-assisted ionization of neutral acceptors, i.e. decreased capture rate as carrier velocity increases. Absence of any sharp increase in current with increasing field argued against any contribution from impact ionization.

Impact ionization in Si:B has been poorly characterized under conditions relevant to generation of inverted hole populations at temperatures below 20 K. In particular, the impact ionization threshold should increase with magnetic field, which can make the conditions more critical. The problem of impact ionization in Si requires further experimental study as a function of concentration, temperature, and magnetic field.

One potential solution to the impact ionization problem is SiGe [13]. The ionization energy of B decreases from 46 meV pure Si to 31 meV with just 4% Ge composition in single crystal SiGe [23]. An additional 2 meV shift is observed when the sample temperature is increased from 4.2 K to 34 K, which does not occur in pure crystal Si. The ionization energy is independent of applied magnetic field up to 11 T. Thus, for SiGe:B with 4% Ge, the impact ionization threshold is reduced to  $E_i = 46$  meV, which is sufficiently less than the optical phonon energy to allow impact ionization. This is a strong argument in favor of  $\text{Si}_{0.96}\text{Ge}_{0.04}$  as the active crystal for a Si-based hot-hole laser. Moreover, SiGe epitaxy by CVD is a well developed growth technology, which encourages consideration of the multilayer periodic doping concept.

Epitaxially grown Si/p-Si devices with periodic doping profiles (Fig. 4) should be considered, as has been done for Ge [8-10]. The main advantage of growing such a device in Si is that the expected substantial gain increase may overcome the challenges associated with bulk Si. Additional advantages are better thermal management and integration with standard Si electronics. Thick epitaxial growth can be achieved by CVD for both Si and SiGe. Wavelengths of emission from 30 to 200  $\mu\text{m}$  appear feasible. Silicon technology offers the possibility of constructing a terahertz transceiver on a single silicon chip. The multilayer p-type Si or SiGe THz laser could be integrated with a SiGe/Si quantum-well infrared photodetector (a shallow-well device with THz response) along with electronics that could drive and modulate the laser and preamplify the detector output.

## GALLIUM ARSENIDE TERAHERTZ LASER

GaAs is a potential active medium for hot-hole THz lasers. Monte Carlo simulations have shown that bulk uniformly-doped GaAs should have acceptable performance [24]. However, due to doubled impurity scattering rate (a consequence of lower dielectric constant) in GaAs relative to Ge, THz gain in p-GaAs devices is expected to be lower than in the well-established p-Ge lasers. Performance of p-GaAs hot-hole lasers would be improved [8-11] by the periodic doping scheme [8-11], by which impurity scattering is eliminated from the active region. This device concept can be applied directly to GaAs.

GaAs is an attractive material for use in hot hole THz lasers due to the potential for periodically-doped multi-layer stacks with thicknesses greater than 800  $\mu\text{m}$ . We expect superior performance for such a laser relative to one using Ge. For instance, a free-standing 800  $\mu\text{m}$  thick active crystal would have losses below  $0.1 \text{ cm}^{-1}$ , which would allow laser action even with very low gain. Single crystal GaAs is known from our intracavity laser absorption experiments to have low THz loss [25]. Here, mm-thick slabs of GaAs were placed inside the cavity of a p-Ge laser, which itself has low gain at the level of  $0.01$ - $0.1 \text{ cm}^{-1}$ . This passive GaAs had no effect on the p-Ge laser performance.

Thick epitaxial GaAs is possible by hydride vapor phase epitaxy (HVPE), which can achieve much faster growth rates than the more widespread GaAs epitaxial growth methods (molecular beam epitaxy or organometallic vapor phase epitaxy). We have demonstrated growth rates well above 100  $\mu\text{m/hr}$  for homoepitaxial GaAs via HVPE in a custom-built reactor at the Air Force Hanscom Research Site [26]. The system consists of a horizontal quartz tube, heated by a three-zone furnace and sealed to allow lowpressure operation in the range of 1 to 5 torr. HCl vapor passing over a liquid Ga source reacts to form GaCl, which is transported to the substrate. Arsenic is supplied in the form of arsine ( $\text{AsH}_3$ ), which decomposes on the surface. Both the Ga source and the substrate are heated to temperatures in the range of 650 to 750°C; the temperature gradient along the tube drives GaCl formation at the source and GaAs deposition on the substrate. The growth rate can be controlled by varying the vapor supersaturation – i.e., increasing or decreasing the partial pressures of the reactants with respect to their equilibrium values alters

the tendency toward growth or etching of GaAs. This control allows us to achieve very rapid epitaxial growth rates, making the growth of periodically-doped multi-layer stacks of thicknesses of at least 800  $\mu\text{m}$  feasible.

The proposed p-GaAs/GaAs multilayer device would have the additional advantage over MBE-grown AlGaAs-GaAs quantum cascade lasers by being tunable over a wide range (1-4 THz). This is due to the inherently broad gain bandwidth of the intervalence band mechanism. QCLs may be temperature tuned by at most  $1\text{ cm}^{-1}$ . In the proposed delta-doped GaAs structures the desired variations in the concentrations of light and heavy holes over the doping period will be more pronounced than in Ge devices due to polar optical phonon scattering. The result will be a comparatively high concentration of light holes in the undoped layers. Therefore, the expected improvement in going from uniform bulk crystal to multilayer structure, already noted for Ge [8-11], should be more significant in GaAs.

Compared with Ge, GaAs has additional factors of polar optical phonon and acoustic piezoelectric phonon scattering processes. The latter is usually unimportant, but the polar optical phonon scattering has a significant role. Some first Monte Carlo simulation results for bulk GaAs, obtained by us, illustrate these features. Distribution functions have been calculated for GaAs and compared with results for Ge in Fig. 8. As expected, a "hard roof" for heavy holes is observed at the optical phonon energy in GaAs. Light holes are born with comparatively low energies in GaAs, where they are more susceptible to ionized impurity scattering. However, integrated over energy, the inversion is very strong compared to Ge, and about 35% of the holes are light. (This constitutes a strong inversion due to the higher density of states in the heavy hole band.) The accumulation of light holes at relatively low energies favors optical emission at lower THz frequencies, which is more advantageous for applications due to higher atmospheric transparency.

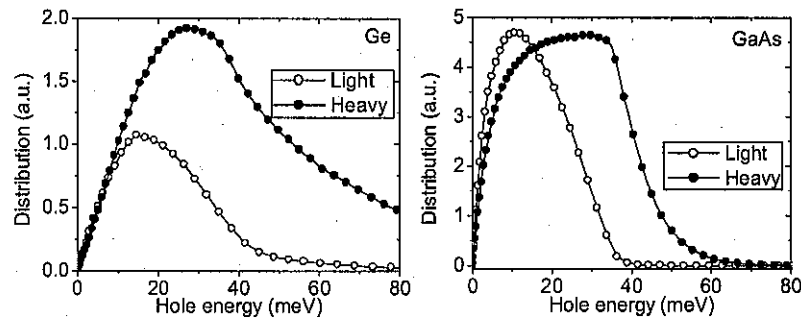


Fig. 8. (Left) Hole distributions for p-Ge in crossed electric and magnetic fields. (Right) Hole distributions for p-GaAs under the same field, temperature, and doping conditions. The optical phonon energy is 37 and 36 meV in Ge and GaAs, respectively. Simulation parameters for both materials:  $T = 20\text{ K}$ ,  $E = 4\text{ kV/cm}$ ,  $B = 3\text{ T}$ ,  $p = 2.5 \times 10^{14}\text{ cm}^{-3}$ .

Calculated gain spectra are compared for bulk uniformly doped Ge and GaAs in Fig. 9. Compared with Ge, GaAs gain peaks at lower wavenumbers, as suggested by the distribution functions Fig. 8. The two curves in Fig. 9 were calculated for the same temperature and applied field magnitudes. The optimal ratio of fields and their magnitudes must be different for two materials according to [24]. Therefore, it is likely possible to find field strengths that allow gain to be somewhat higher in GaAs than what is plotted in Fig. 9.

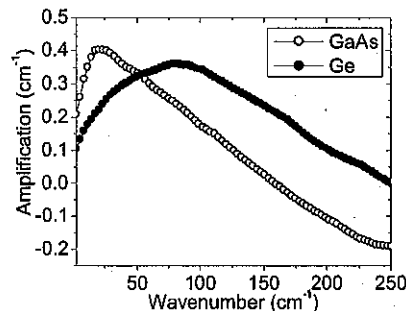


Fig. 9. Calculated gain spectra for bulk p-Ge and p-GaAs. Simulation parameters for both materials:  $T = 20\text{ K}$ ,  $E = 4\text{ kV/cm}$ ,  $B = 3\text{ T}$ ,  $p = 2.5 \times 10^{14}\text{ cm}^{-3}$ .

A factor that affects GaAs is the 2-fold difference in direct intersubband transition matrix elements between light and heavy hole bands. Fig. 10 compares the normalized matrix elements plotted as a function of crystallographic direction in the same scale for comparison (calculated in 4 x 4 Hamiltonian with valence band parameters  $L = -30.4$ ,  $M = -5.7$ ,  $N = -33.9$  for Ge and  $L = -16.0$ ,  $M = -3.5$ ,  $N = -17.3$  for GaAs). Averaged over directions, the matrix elements are 5.85 for GaAs and 11.5 for Ge. This factor is already included in Fig. 9, where it is seen that despite higher degree of inversion, the gain coefficients (ignoring free carrier absorption) have similar magnitude in Ge and GaAs.

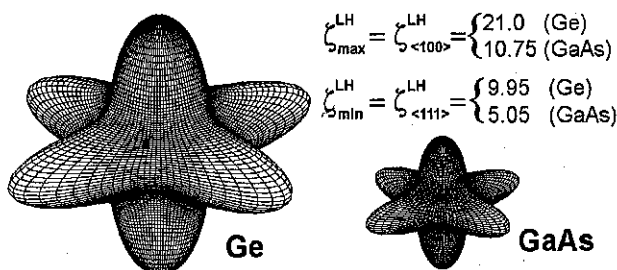


Fig. 10. Calculated intersubband optical matrix elements for Ge (left) and GaAs (right).

### SUMMARY

This paper briefly summarized the mechanisms of inversion that can produce THz lasing in p-Ge based on hot-hole dynamics in applied electric and magnetic fields. The recent innovation of a multilayer periodically doped p-Ge/Ge structure that can give higher gain, and therefore higher duty and operating temperature, was summarized. The prospects and challenges for a hot hole THz laser in Si were presented, with the suggestion that a multilayer periodically doped p-Si/Si or p-SiGe/SiGe may be the best route to success. Finally, hot hole lasing in p-GaAs and GaAs/p-GaAs structures was discussed.

### ACKNOWLEDGMENTS

This work was supported in part by a ASEE/AFOSR summer faculty fellowship to R. E. Peale and by a grant from AFRL/SNHC at Hanscom AFB, MA. Work by AFRL authors was funded by the US Air Force Office of Scientific Research.

### REFERENCES

1. E. Bründermann, "Widely Tunable Far-Infrared Hot-Hole Semiconductor Lasers" in *Long wavelength infrared semiconductor lasers*, edited by H. K. Choi (Wiley, NJ, 2004), pp. 279-343.
2. S. G. Pavlov, Kh. Zhukavin, E. E. Orlova, V. N. Shastin, A. V. Kirsanov, H.-W. Huebers, K. Auien and H. Riemann, "Stimulated emission from donor transitions in silicon", *Phys. Rev. Lett.* **84**, 5220, 2000.
3. B. S. Williams, H. Callebaut, S. Kumar, Q. Hu and J. L. Reno, "3.4 THz quantum cascade laser based on longitudinal-optical-phonon scattering for depopulation", *Appl. Phys. Lett.* **82**, 1015, 2003.
4. R. Kohler, A. Tredicucci, F. Beltram, H. E. Beere, E. H. Linfield, A. G. Davies, D. A. Ritchie, R. C. Iotti, and F. Rossi, "Terahertz semiconductor-heterostructure laser", *Nature* **417**, 156, 2002.
5. M. Rochat, L. Ajili, H. Willenberg, J. Faist, H. Beere, G. Davies, E. Linfield, and D. Ritchie, "Low-threshold terahertz quantum-cascade lasers", *Appl. Phys. Lett.* **81**, 1381, 2002.
6. R. Bates, S. A. Lynch, D. J. Paul, Z. Ikonik, R. W. Kelsall, P. Harrison, S. L. Liew, D. J. Norris, A. G. Cullis, W. R. Tribe, and D. D. Arnone, "Interwell intersubband electroluminescence from Si/SiGe quantum cascade emitters", *Appl. Phys. Lett.* **83**, 4092, 2003.
7. R. Brazis and F. Keilmann, "Lattice absorption of Ge in the far infrared", *Solid State Comm.* **70**, 1109, 1989.



8. M. V. Dolguikh, A. V. Muravjov, and R. E. Peale, "Intravalence-band THz laser in selectively-doped semiconductor structure", in *Novel In-Plane Semiconductor lasers III*, edited by C. F. Gmachl and D. P. Bour, Proc. SPIE **5365**, 184, 2004.
9. M. V. Dolguikh, A. V. Muravjov, and R. E. Peale, "Selectively doped germanium THz laser", in *Terahertz for Military and Security Applications*, edited by R. J. Hwu and D. L. Woolard, Proc. SPIE **5411**, 207, 2004.
10. M. V. Dolguikh, A. V. Muravjov, and R. E. Peale, "Monte Carlo simulation of multilayer delta doped germanium THz laser", in *Proc. Numerical Simulation of Optoelectronic Devices*, edited by J Piprek and S Li, IEEE Lasers and Electro-Optics Society, pp. 97-98, Piscataway, NJ, 2004.
11. M. V. Dolguikh, A. V. Muravjov, R. E. Peale, M. Klimov, O. A. Kuznetsov, and E. A. Uskova, "Terahertz gain on intersubband transitions in multilayer delta-doped p-Ge structures", *J. Appl. Phys.* **98**, 1 in press, 2005.
12. Peter Bruesch, *Phonons: Theory and Experiments II: Experiments and Interpretation of Experimental Results (Phonons)*, p. 57, Springer, Berlin, 1987.
13. E. Bruendermann, E. E. Haller, A. V. Muravjov, "Terahertz emission of population-inverted hot-holes in single-crystalline silicon", *Appl. Phys. Lett.* **73**, 723 1998.
14. V. I. Gavrilenko, E. P. Dodin, Z. F. Krasil'nik, and M. D. Chernobrovtsseva, *Sov. Phys. Semicond.* **21**, 299, 1987.
15. E. V. Starikov and P. N. Shiktorov, "Numerical simulation of far infrared emission under population inversion of hot sub-bands", *Opt. Quantum Electron.* **23**, S177, 1991.
16. A. V. Muravjov, R. C. Strijbos, W. Th. Wenckebach and V. N. Shastin, "Population Inversion of Landau Levels in the Valence Band of Silicon in Crossed Electric and Magnetic Fields", *Phys. Stat. Solidi. (b)* **205**, 575, 1998.
17. G. L. Bir and G. E. Pikus, *Symmetry and strain-induced effects in semiconductors*, Wiley, NY, 1974.
18. F. M. Bufler, A. Schenk, and W. Fichtner, "Simplified model for inelastic acoustic phonon scattering of holes in Si and Ge", *J. Appl. Phys.* **90**, 2626 2001.
19. E. Rosencher, V. Mosser, and G. Vincent, "Transient-current study of field-assisted emission from shallow levels in silicon", *Phys. Rev. B* **29**, 1135, 1984.
20. B. K. Ridley, *Quantum Processes in Semiconductors*, Oxford, NY, 1999.
21. W. Kaiser and G. H. Wheatley, "Hot electrons and carrier multiplication in silicon at low temperature", *Phys. Rev. Lett.* **3**, 334, 1959.
22. R. E. Larrabee, "High-Field effect in boron-doped silicon", *Phys. Rev.* **116**, 300, 1959.
23. X. H. Shi, P. L. Liu, Z. H. Chen, S. C. Shen, and J. Schilz, "Photoconductivity spectra for boron acceptors in Si<sub>1-x</sub>Ge<sub>x</sub> alloys", *Appl. Phys. Lett.* **68**, 211, 1996.
24. P. Kinsler and W. Th. Wenckebach, "Hot-hole lasers in III-V semiconductors", *J. Appl. Phys.* **90**, 1692, 2001.
25. E. W. Nelson, S. H. Withers, A. V. Muravjov, R. C. Strijbos, R. E. Peale, S. G. Pavlov, V. N. Shastin, and C. J. Fredricksen, "High-resolution study of composite cavity effects for p-Ge laser", *IEEE J. Quantum Electronics* **37**, 1525, 2001.
26. D. Bliss, C. Lynch, D. Weyburne, K. O'Hearn, and J. Bailey, "Epitaxial Growth of Thick GaAs on a Patterned Wafer for NLO Applications", submitted to *J. Crystal Growth*.

